

Formation Sequence of Lead Platinum Interfacial Phases in Chemical Solution Deposition Derived $\text{Pb}(\text{Zr}_{1-x}\text{Ti}_x)\text{O}_3$ Thin Films

Ann-Christin Dippel,[†] Theodor Schneller,^{*,†}
Rainer Waser,[†] Daesung Park,[‡] and Joachim Mayer[‡]

[†]*Institut für Werkstoffe der Elektrotechnik II (IWE II) and*
[‡]*Gemeinschaftslabor für Elektronenmikroskopie (GFE),*
RWTH Aachen University, D- 52056 Aachen, Germany

Received April 28, 2010

Revised Manuscript Received November 4, 2010

Among the large variety of electroceramic thin film materials, lead zirconate titanate (PZT) stands out because of excellent piezoelectric and ferroelectric performance. Hence, it is applied in devices such as actuators in micro or nano electromechanical systems (MEMS/NEMS) and ferroelectric random access memories (FeRAM).^{1,2} Chemical solution deposition (CSD) is an established processing technique to fabricate PZT thin films.³ Most CSD approaches to deposit PZT layers reported in the literature are sol–gel routes, starting from lead acetate, titanium, and zirconium alkoxides, and an (alkoxy) alcoholic solvent. It is known how to successfully control the microstructure and the electrical properties of the films, but the underlying mechanisms of nucleation and growth are not yet fully understood.

With regard to texture evolution in PZT coatings on common platinized silicon substrates of the layer sequence Pt/Ti/SiO₂/Si or Pt/TiO₂/SiO₂/Si, different models on the dominant factors have been postulated as discussed, e.g., by Brooks et al. and Norga and Fe.^{4,5} These include (i) the preannealing of the substrate, leading to the formation of platinum hillocks, (ii) crystallization via a kinetically favored fluorite or pyrochlore phase which shows a similar near-range order as the amorphous gel, (iii) the diffusion of titanium atoms upon substrate preannealing from the adhesion layer through the electrode to the Pt surface where they act as nucleation seeds, and (iv) the occurrence of an intermediate lead platinum phase at the electrode film interface in a certain temperature regime below the crystallization temperature, similar to Pt–Bi alloy formation in strontium bismuth tantalate films.⁶ The models suggesting Ti diffusion and a transient Pt_xPb

phase, respectively, account for the frequently obtained preferred (111) orientation and columnar morphology of the PZT films based on the small mismatch between the (111) lattice planes of Pt on the one hand and either PbTiO₃ (as Ti enriched PZT) or Pt_xPb on the other. Concerning the intermetallic lead platinum phase, different stoichiometries have been found in EDX analysis: Chen and Chen⁷ detected a Pt/Pb molar ratio of 5–7, whereas Huang et al.⁸ and Kaewchinda and co-workers⁹ concluded the composition Pt₃Pb and Pt_{3–4}Pb, respectively. The primary condition for the formation of the intermetallic phase in general was identified to be a reduced partial pressure of oxygen at the film substrate interface.⁴

Because the chemistry and the processing parameters involved in the cited studies varied substantially, a direct comparison of the results does not implicitly lead to meaningful conclusions. The fact that the investigated PZT compositions range from 30 to 65% Zr content further adds to this inconsistency. However, the lead titanate portion is believed to be the driving component in the nucleation process of the perovskite phase because of its lower crystallization temperature.¹⁰ Therefore, this study deals with the analysis of transient phases in pure PbTiO₃ layers during annealing and compares the results to PZT layers of the Zr/Ti molar ratios 30/70 and 45/55, which are particularly relevant for ferroelectric and piezoelectric applications, respectively. All samples were prepared by the same CSD route in order to ensure the significance of the findings. The main focus was on the lead platinum interaction at the film substrate interface while the other mentioned mechanisms (i) to (iii) played a subordinate role owing to the particular processing parameters: (i) the surface roughness of the platinum electrode had been enhanced by optimizing the sputter deposition process;⁴ (ii) fluorite phase formation, which actually only occurs to considerable extent in Zr rich PZT, was suppressed by a 15% excess of the lead compound in the precursor solutions;¹¹ and (iii) the choice of titanium oxide instead of metallic titanium as adhesion layer between the electrode and the silicon wafer prohibited titanium diffusion and oxidation within and on top of the electrode while preconditioning the substrates.¹²

The chosen CSD route is described in detail in earlier works.^{11,13} Briefly summarized, it comprises dried lead

*Corresponding author. E-mail: schneller@iwe.rwth-aachen.de.

- (1) Murali, P. *J. Nanosci. Nanotechnol.* **2008**, 8, 1560–1567.
- (2) Scott, J. F. *Science* **2007**, 315, 954–959.
- (3) Schneller, T.; Majumder, S. B.; Waser, R. *Ceramics Science and Technology*; Riedel, R., Chen, I.-W., Eds.; Wiley-VCH: Weinheim, Germany, 2008; Vol. 1, Chapter 11, pp 443–509.
- (4) Brooks, K. G.; Reaney, I. M.; Klissurska, R.; Huang, Y.; Bursill, L.; Setter, N. *J. Mater. Res.* **1994**, 9, 2540–2543.
- (5) Norga, G. J.; Fe, L. *Mater. Res. Soc. Symp. Proc.* **2001**, 655, CC9.1.1–CC9.1.11.
- (6) Calzada, M. L.; Gonzalez, A.; Garcia-Lopez, J.; Jimenez, R. *Chem. Mater.* **2003**, 15, 4775–4783.

- (7) Chen, S.-Y.; Chen, I.-W. *J. Am. Ceram. Soc.* **1998**, 81, 97–105.
- (8) Huang, Z.; Zhang, Q.; Whatmore, R. W. *J. Mater. Sci. Lett.* **1998**, 17, 1157–1159.
- (9) Kaewchinda, D.; Chairaungsri, T.; Naksata, M.; Milne, S. J.; Brydson, R. *J. Eur. Ceram. Soc.* **2000**, 20, 1277–1288.
- (10) Wilkinson, A. P.; Speck, J. S.; Cheetham, A. K. *Chem. Mater.* **1994**, 6, 750–754.
- (11) Schneller, T.; Waser, R. *J. Sol–Gel Sci. Technol.* **2007**, 42, 337–352.
- (12) Sreenivas, K.; Reaney, I.; Maeder, T.; Setter, N.; Jagadish, C.; Elliman, R. G. *J. Appl. Phys.* **1994**, 75, 232–239.
- (13) Dippel, A.-C.; Schneller, T.; Waser, R. *Integr. Ferroelectr.* **2008**, 98, 3–10.

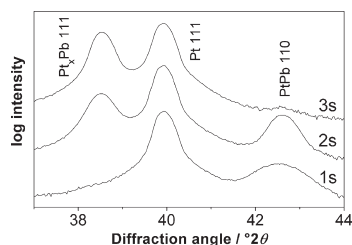


Figure 1. XRD patterns (Cu K α radiation) of undiluted PbTiO₃ precursor solution layers after heat treatment at 650 °C for the indicated durations, showing the consecutive evolution of the two intermediate lead platinum phases as assigned by refs 14 and 15.

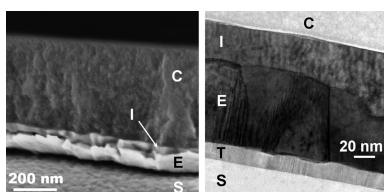


Figure 2. Cross-sectional scanning electron micrograph (left) and bright field TEM image (right) of samples that exhibit the intermediate lead platinum layer; legend: S, SiO₂ substrate; T, TiO₂ adhesion layer; E, Pt electrode; I, intermediate Pt_xPb layer; C, CSD precursor layer.

acetate, titanium, and zirconium alkoxides, and the solvent *n*-butanol which form a sol in a “one-pot” reaction. Different thicknesses of the spin-coated layers were achieved by varying the concentration of the precursor solution between 1 mol L⁻¹ (undiluted stock solution) and 0.2 mol L⁻¹. The wet films underwent quasi-isothermal heat-treatment on laboratory hot plates that provided annealing temperatures between 250 and 700 °C for selective periods ranging from a single second to hours.

Fundamental information about the nature of intermediate phases and the conditions of their appearance was derived from single coatings of the one molar lead titanate precursor solution. This kind of specimens allowed for higher time resolution of the reaction kinetics compared to thinner layers since the course of reaction proceeded more slowly. In principle, two transient phases were recorded in X-ray diffraction scans as illustrated in Figure 1. In the vicinity of the Pt 111 reflection, signals of the 111 reflection of a stoichiometrically unspecified Pt_xPb phase¹⁴ and the 110 reflection of the phase PtPb¹⁵ were identified. These phases developed in dependence on the annealing time as described below. Cross sectional scanning as well as transmission electron micrographs of samples showing the reflections of both lead platinum phases are given in Figure 2. In these images, an interlayer between the electrode and the deposited film up to a thickness of ~50 nm is clearly visible. To specify the stoichiometry factor *x* in Pt_xPb, EDX line scans performed on TEM lamellae were evaluated. The obtained results for the TEM sample of Figure 2 as well as the corresponding HAADF images are presented in Figures 3 and 4. As the different gray scales of the metallic film parallel to its surface (see Figure 3) suggest, the composition of the interlayer varied locally. The two line profiles depict distinct regions of the sample: region

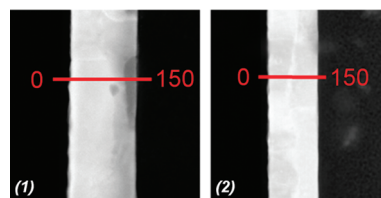


Figure 3. High-angle annular dark field (HAADF) images and EDX scan lines (in nanometers, profiles see Figure 4) of one sample showing the XRD reflections of both PtPb and Pt₃Pb. The different gray scales indicate either a compositional variation or a change in grain structure. Discrimination is possible only by analyzing the EDX signals.

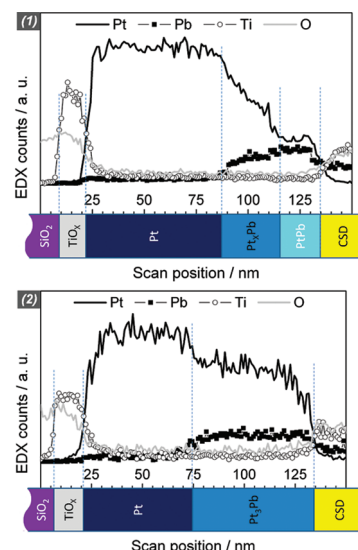


Figure 4. EDX line profiles corresponding to the cross-sectional HAADF images of Figure 3. The profiles map the layer sequence as schematically shown at the bottom. The understoichiometric phase TiO_x of the adhesion layer represents partially crystalline TiO₂ in an amorphous Ti-O matrix.

(1) where ~20 nm of the stoichiometric PtPb phase separate the precursor from an intermetallic layer with gradually increasing Pt content, and region (2) in which an approx. 50 nm thick layer of rather constant Pt/Pb molar ratio of 3 is found in agreement with refs 8 and 9. As a result of the Pb diffusion into the Pt layer, the initial electrode thickness of 100 nm increased by almost 15%. At the same time, the precursor layer showed a certain Pb deficiency in comparison to its Ti content in the proximity of the interface.

Generally, the two intermetallic phases emerged by a fixed sequence (cf. Figure 1). The equimolar composition showed before the Pt₃Pb phase evolved and vanished after a certain period of coexistence, leaving solely the platinum-rich composition. This progression suggested a model of phase evolution as follows: In the initial stage of the annealing, a lead platinum layer developed at the film–substrate contact surface from equal quantities of the two constituents. As the applied elevated temperatures increased the mobility of the atoms, Pb further diffused into the Pt layer where it formed the intermetallic compound in understoichiometric ratio. As the HAADF images revealed, the phase transition from PtPb to Pt₃Pb locally proceeded with

(14) ICDD reference pattern PDF # 6–574.

(15) ICDD reference pattern PDF # 6–374.

different rates leading to a certain inhomogeneity over the electrode area. In grazing incidence XRD measurements, neither of the lead platinum phases was detectable, indicating that they were highly textured. The same conclusion was drawn from the absence of reflections in the entire 2θ scan range of $20\text{--}60^\circ$ except for the ones displayed in Figure 1 even though, in the case of PtPb, the recorded reflection did not correspond to the strongest reflection in the reference pattern.¹⁴

In ref 7, the formation mechanism of the transient lead platinum phase was described in detail. It essentially consists of two steps: first, Pb^{2+} ions are reduced to atomic Pb^0 which subsequently diffuses into the Pt layer. The low oxygen partial pressure close to the interface is created during the burnout of the organic components in the deposited precursor coating. Factors like coating thickness, annealing temperature and duration were found to govern the period of existence of the Pt_xPb phase.^{5,7} These kinetic aspects applied to the route presented in this study as well in that the lead platinum phases prevailed the longer the higher the precursor solution concentration (the thicker the coating), the lower the temperature, and the shorter the duration of the annealing. However, the literature does not include reports on any PtPb interlayer that was demonstrated in this work.

To evaluate the phase formation processes for varying film composition $\text{Pb}(\text{Zr}_{1-y}\text{Ti}_y)\text{O}_3$ ($y = 1, 0.7, 0.55, 0$) the results obtained for single coatings of undiluted stock solutions annealed for 30 s at different temperatures were compared. The temperature-dependent occurrence of the two intermetallic phases under these conditions is illustrated in Figure 5. It is obvious that the decomposition and the correlated reduction of lead ions to lead atoms set in at higher temperatures in the Zr-rich layers. In comparison to pure lead titanate, the lead zirconate component clearly caused a decelerated combustion of the organic components, a behavior that was also reported for bulk gels.¹⁶ Furthermore, the transformation from PtPb to Pt_xPb in the Zr-rich layers passed within a smaller temperature interval. Presumably, the rise in reaction temperatures by $\sim 100^\circ\text{C}$ caused this increase in rate of diffusion.

In the basic examination of the transient phases described above, the coatings were annealed for varying soaking times in the range from 1 s to 60 min at constant temperatures between 250 and 700°C . By contrast, the optimum fabrication conditions for functional PZT films of the applied route involve two separate annealing steps: the rather short pyrolysis at $350\text{--}400^\circ\text{C}$, followed by the crystallization at around 700°C for several minutes.¹¹ Under these standard conditions, the distinct processes of intermediate and perovskite phase formation that were

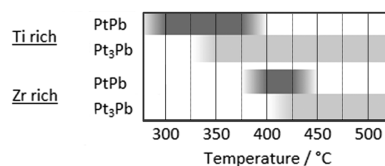


Figure 5. Correlation between the existence of the two lead platinum phases in samples of undiluted precursor solution layers heated for 30 s at the indicated temperatures. “Ti rich” represents the results found for pure PbTiO_3 as well as PZT layers with a Zr content of 30%, “Zr rich” indicates the findings for pure PbZrO_3 and PZT layers with Zr/Ti ratio of 45/55.

observable in the thick coatings are supposed to take place coinstantaneously to some extent during the second phase of thermal treatment. In this way, the transfer of the Pt [111] texture via the intermediate (111) Pt_3Pb layer to the PZT film is plausible. The conventional deposition parameters of PZT films include repeated spin-on of coatings each several tens of nanometers thick.^{11,17} Advanced PbTiO_3 layers,¹³ however, prepared as stacks of individual 25–30 nm thick coatings lacked the preferred (111) orientation common for PZT. Likewise, Ellerkmann et al.¹⁸ recently reported on the loss of the (111) orientation in PZT films thinner than the standard. Evidently, there is a trend that the texture transfer ceases with decreasing coating thickness. Yet, the (111) texture was re-established in very thin coatings when their heating was performed in reducing atmosphere which enhanced the duration of the Pt_3Pb phase by extrinsically adjusted, steady low oxygen partial pressure.¹⁸ On the basis of the findings presented above, it is assumed that preferred or non-preferred orientation results from the decomposition kinetics rather than the presence or absence of zirconium. The fact that Zr-rich layers develop the intermetallic phases not until higher temperatures apparently plays only a subordinate role compared to other factors such as the coating thickness.

In summary, this study verified the formation of a lead platinum interlayer of composition Pt_3Pb when heat-treating sol–gel PbTiO_3 thin films on conventional $\text{Si}/\text{SiO}_2/\text{TiO}_2/\text{Pt}[111]$ substrates that had previously been observed in comparable routes to PZT. Unless the annealing atmosphere was oxygen-depleted, the thickness of the individual coatings primarily determined whether the [111] texture transfer from the Pt_3Pb layer to the perovskite film took place. Basically, the decomposition kinetics exerted the major influence in this regard compared with the actual composition of the PZT system. For the first time, the evolution of the Pt_3Pb layer was found to be preceded by the formation of a thin layer of equimolar composition PtPb at the very contact surface between the deposited precursor coating and the electrode.

(16) Feth, M. P.; Weber, A.; Merkle, R.; Reinohl, U.; Bertagnolli, H. *J. Sol–Gel Sci. Technol.* **2003**, 27, 193–204.

(17) Schneller, T.; Kohlstedt, H.; Petraru, A.; Waser, R.; Guo, J.; Denlinger, J.; Learmonth, T.; Glans, P.-A.; Smith, K. E. *J. Sol–Gel Sci. Technol.* **2008**, 48, 239–252.

(18) Ellerkmann, U.; Schneller, T.; Nauenheim, C.; Boettger, U.; Waser, R. *Thin Solid Films* **2008**, 516, 4713–4719.